Porphyrin Nanotubes Based on Self-Assembly of Mo(V)−Dodecaphenylporphyrin Complexes and Inclusion of Mo−Oxo Clusters: Synthesis and Characterization by X-ray Crystallography and Transmission Electron Microscopy

Takahiko Kojima,*[,†,‡] Ryosuke Harada,[†,||] Tatsuaki Nakanishi,[†] Kenji Kaneko,[§] and Shunichi Fukuzumi[⊥]

Department of Chemistry, Faculty of Sciences, and The Research Laboratory for High Voltage Electron Microscopy, Kyushu University, Hakozaki, Higashi-Ku, Fukuoka 812-8581, and Department of Material and Life Science, Graduate School of Engineering, Osaka University, SORST, Japan Science and Technology Agency (JST), 2-1 Yamadaoka, Suita, Osaka 565-0871, Japan

Received August 28, 2006. Revised Manuscript Received September 28, 2006

A saddle-distorted molybdenum(V)−dodecaphenylporphyrin (H_2DPP) complex, [Mo(DPP)(O)(OMe)] (**1**), was converted to $[Mo(DPP)(O)(H_2O)]^+$ (**2**) in the course of recrystallization from toluene with vapor diffusion of methanol. The complex **2** was organized via self-assembly to form a porphyrin nanotube having a diameter of 1 nm, concomitant with size-selective inclusion of three kinds of novel tetranuclear Mo(VI)−oxo clusters in the nanotube. This porphyrin nanotube exhibits amphiphilic characteristics, that is, a hydrophobic porphyrin surface and a hydrophilic inner-sphere made of aquo ligands to include ionic and hydrophilic entities. Each nanotube has no direct interaction; however, the toluene molecules of crystallization linked the nanotubes together with intermolecular $\pi-\pi$ and CH/π interactions. Transmission electron microscopy measurements and energy-dispersive X-ray analysis revealed that the diameters of porphyrin nanotubes could be altered by the size of the Mo−oxo clusters included and also a porphyrin nanoring could be obtained. These results indicate that a variety of porphyrin nanotubular structures can be fabricated by using DPP complexes via cooperatively template-assisted self-assembly.

Introduction

Nanomaterials derived from self-assembly of functional molecules have attracted much attention due to their flexibility of structures to be obtained.[1−6] Benefits of self-assemblies are (1) self-recombination toward the global minimum to afford uniform shape selectively and (2) ordering of each molecular unit in one direction.[7] In the presence of template molecules including small organic and inorganic molecules and also macromolecules, the size and shape of the aggregates can be more strictly regulated in a defined manner.

Porphyrins and metalloporphyrins have been recognized as attractive building blocks of supramolecular assemblies toward construction of functional materials.[8−10] In nature, an efficient photovoltaic process can be achieved as photosynthesis by bacteriochlorophylls, in which a large magnesium−porphyrin assembly acts as the light-harvesting antenna to conduct light energy conversion to generate gradients of electrical potentials to perform successive electron transfer toward the production of dioxygen and ATP.[11]

Metalloporphyrin assemblies have been investigated as models of the light-harvesting antenna complexes.[12−14] Along

* To whom correspondence should be addressed. E-mail: kojima@chem.eng.osaka-u.ac.jp.
† Department of Chemistry, Kyushu University.
‡ Present address: Department of Material and Life Science, Graduate School of Engineering, Osaka University, Japan Science and Technology Agency (JST), 2-1 Yamadaoka, Suita, Osaka 565-0871, Japan.
§ The Research Laboratory for High Voltage Electron Microscopy, Kyushu University.
|| Present address: Center for Future Chemistry, Kyushu University, 744 Motooka, Fukuoka 819-0395, Japan.
⊥ Osaka University.

(1) Cao, G. *Nanostructures and Nanomaterials: Synthesis, Properties and Applications*; Imperial College Press: London, 2004.
(2) *Handbook of Nanotechnology*; Bhushan, B., Ed.; Springer: Berlin, 2004.
(3) (a) Hill, J. P.; Jin, W.; Kosaka, A.; Fukushima, T.; Ichihara, H.; Shimomura, T.; Ito, K. Hashizume, T.; Ishii, N.; Aida, T. *Science* **2004**, *304*, 1481. (b) Verbiest, T.; Elshocht, S. V.; Kauranen, M.; Hellemans, L.; Snauwaert, J.; Nuckolls, C.; Katz, T. J.; Persoons, A. *Science* **1998**, *282*, 913.
(4) (a) Burda, C.; Chen, X.; Narayanan, R.; El-Sayed, M. A. *Chem. Rev.* **2005**, *105*, 1025. (b) Daniel, M.-C.; Astruc, D. *Chem. Rev.* **2004**, *104*, 293.
(5) (a) Thomas, K. G.; Kamat, P. V. *Acc. Chem. Res.* **2003**, *36*, 888. (b) Shenhar, R.; Rotello, V. M. *Acc. Chem. Res.* **2003**, *36*, 549. (c) Sastry, M.; Rao, M.; Ganesh, K. N. *Acc. Chem. Res.* **2002**, *35*, 847. (d) Templeton, A. C.; Wuelfing, W. P.; Murray, R. W. *Acc. Chem. Res.* **2000**, *33*, 27.
(6) (a) Kamat, P. V. *J. Phys. Chem. B* **2002**, *106*, 7729. (b) Niemeyer, C. M. *Angew. Chem., Int. Ed.* **2003**, *42*, 5796.
(7) Whitesides, G. M.; Grzybowski, B. *Science* **2002**, *295*, 2418.
(8) (a) Okada, S.; Segawa, H. *J. Am. Chem. Soc.* **2003**, *125*, 2792. (b) Iverson, B. L.; Shreder, K.; Kral, V.; Sansom, P.; Lynch, V.; Sessler, J. L. *J. Am. Chem. Soc.* **1996**, *118*, 1608.
(9) Hu, J.-S.; Guo, Y.-G.; Liang, H.-P.; Wan, L.-J.; Jiang, L. *J. Am. Chem. Soc.* **2005**, *127*, 17090.
(10) Hasobe, T.; Fukuzumi, S.; Kamat, P. V. *J. Am. Chem. Soc.* **2005**, *127*, 11884.
(11) (a) *The Photosynthetic Reaction Center*; Deisenhofer, J., Norris, J. R., Eds.; Academic Press: San Diego, 1993. (b) *Anoxygenic Photosynthetic Bacteria*; Blankenship, R. E., Madigan, M. T., Bauer, C. E., Eds.; Kluwer Academic Publishing: Dordrecht, 1995.
(12) (a) Kim, D.; Osuka, A. *Acc. Chem. Res.* **2004**, *37*, 735. (b) Hwang, I.-W.; Kamada, T.; Ahn, T. K.; Ko, D. M.; Nakamura, T.; Tsuda, A.; Osuka, A.; Kim, D. *J. Am. Chem. Soc.* **2004**, *126*, 16187. (c) Stang, P. J.; Olenyuk, B. *Acc. Chem. Res.* **1997**, *30*, 502.

10.1021/cm062031k CCC: $37.00
Published on Web 11/22/2006

this line, Kobuke and Takahashi have reported the preparation of a circular Zn(II)−porphyrin assembly with ∼40 nm diameter by using complementary coordination.[15] Exploration has just started, however, to discover the possibility of porphyrins, metalloporphyrins, and their assemblies to exhibit various functionalities as materials and supramolecules. To date, porphyrin-based nanostructures have been exemplified to be rods,[16] rings,[14,17] particles,[18] sheets,[19] wires,[20] and tubes.[21] Those structures have been prepared with or without templates, rather formed by virtue of J-aggregation[22] due to intermolecular $\pi-\pi$ interactions of planar porphyrins and metalloporphyrins. Metalloporphyrin-based functional materials have been represented by porous materials reported by Suslick and co-workers, consisting of Co(III)(porphyrin)−Co(II) trinuclear clusters, to exhibit selective and reversible absorption properties toward various organic molecules.[23] In addition, Aida and co-workers have reported on "porphyrin peapods", in which fullerenes are included in the inner space of the tubular Zn(II)−porphyrin assembly with use of intermolecular hydrogen bonding.[24] It may be possible to create various shapes and sizes of assemblies in a similar strategy to encapsulate and/or include external molecules; however, robust and planar structures of porphyrins will limit the divergence of structural features of porphyrin supramolecules. Thus, new concepts are desired to construct porphyrin nanostructures in a well-regulated and well-organized manner.

In order to explore the abundant possibility of porphyrin nanostructures toward the innovation of new functional materials, we can choose different types of building blocks other than the usual planar porphyrins. As a candidate of such building blocks, we have focused on saddle-distorted porphyrins and metalloporphyrins, which provide *curved surfaces*, allowing us to access novel morphology of porphyrin nanostructures. Such curved surfaces would give circular and/or tubular nanostructures as a result of their self-assembly based on noncovalent interactions as shown in Scheme 1. In order to realize such a curved surface, we have focused on dodecaphenylporphyrin (H_2DPP), which has been known to exhibit a large saddle distortion.[25]

Scheme 1. Formation of Unique Shapes Based on Self-Assembly of Building Blocks with a Curved Surface

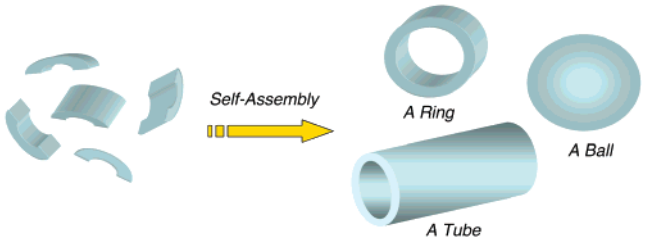

We report herein preparation of a novel "porphyrin nanotube" with $[Mo^{V}(DPP)(O)(H_2O)]^{+}$ as a building block by taking advantage of the unique shape of the saddle-distorted porphyrin complexes via their self-assembly and transmission electron microscopy (TEM) observations of larger Mo(V)−DPP nanotubes which form a porphyrin nanoring of ∼200 nm in diameter.[26]

Experimental Section

Materials. PhOH was distilled under reduced pressure. Toluene used for crystallization was purified by successive treatment with concentrated H_2SO_4, H_2O, NaOH(aq), and H_2O, dried with anhydrous $CaCl_2$, and then distilled from a sodium-benzophenone ketyl solution. CH_2Cl_2 for spectroscopic measurements was distilled from CaH_2. All other chemicals were of reagent grade. H_2DPP was prepared by cross-coupling reaction between phenylboronic acid and 2,3,7,8,12,13,17,18-octabromo-5,10,15,20-tetraphenylporphyrin, according to the procedures described by Che et al.[27] Elemental analysis data for all compounds were obtained at the Service Center of the Elemental Analysis of Organic Compounds, Department of Chemistry, Kyushu University.

Preparation of [Mo(DPP)(O)(OMe)] (1). H_2DPP (0.100 g, 0.082 mmol) was heated with $Mo(O)_2(acac)_2$ (0.134 g, 0.410 mmol) in PhOH (0.5 g) at 240 °C under nitrogen for 2 h. After the removal of PhOH under reduced pressure, the residue was chromatographed on an alumina column using CH_2Cl_2/MeOH (10:1) and a silica gel column using CH_2Cl_2/MeOH (1:1) as the eluent. The second green fraction was collected. The crystallization from CH_2Cl_2/MeOH (1:1) gave **1** as a green powder (0.047 g, 41%). Elem anal. Calcd for $C_{93}H_{63}Mo_1N_4O_2{\cdot}CH_3OH$: C, 80.85; H, 4.84; N, 4.01. Found: C, 80.45; H, 4.67; N, 4.00.

Preparation of $[Mo(DPP)(O)(H_2O)](Mo_4O_{14}H_2)_{0.4}(Mo_4O_{13}H_2)_{0.1}{\cdot}1.2H_2O{\cdot}0.5C_7H_8$ (2). Green crystals of the porphyrin nanotube (**2**)

(13) (a) Imamura, T.; Fukushima, K. *Coord. Chem. Rev.* **2000**, *198*, 133. (b) Wojaczyski, J.; Latos-Grazyski, L. *Coord. Chem. Rev.* **2000**, *204*, 113.
(14) Lensen, M. C.; Takazawa, K.; Elemans, J. A. A. W.; Jeukens, C. R. L. P. N.; Christianen, P. C. M.; Maan, J. C.; Rowan, A. E.; Nolte, R. J. M. *Chem.−Eur. J.* **2004**, *10*, 831.
(15) Takahashi, R.; Kobuke, Y. *J. Am. Chem. Soc.* **2003**, *125*, 2372.
(16) (a) Yuasa, M.; Oyaizu, K.; Yamaguchi, A.; Kuwakado, M. *J. Am. Chem. Soc.* **2004**, *126*, 11128. (b) Schwab, A. D.; Smith, D. E.; Rich, C. S.; Young, E. R.; Smith, W. F.; de Paula, J. C. *J. Phys. Chem. B* **2003**, *107*, 11339. (c) Schwab, A. D.; Smith, D. E.; Bond-Watts, B.; Johnston, D. E.; Hone, J.; Johnson, A. T; de Paula, J. C.; Smith, W. F. *Nano Lett.* **2004**, *4*, 1261.
(17) Jeukens, C. R. L. P. N.; Lensen, M. C.; Wijnen, F. J. P.; Elemans, J. A. A. W.; Christianen, P. C. M.; Rowan, A. E.; Gerritsen, J. W.; Nolte, R. J. M.; Maan, J. C. *Nano Lett.* **2004**, *4*, 1401.
(18) Gong, X.; Milic, T.; Xu, C.; Batteas, J. D.; Drain, C. M. *J. Am. Chem. Soc.* **2002**, *124*, 14290.
(19) (a) Milic, T. N.; Chi, N.; Yablon, D. G.; Flynn, G. W.; Batteas, J. D.; Drain, C. M. *Angew. Chem., Int. Ed.* **2002**, *41*, 2117. (b) Milic, T.; Garno, J. C.; Batteas. J. D.; Smeureanu, G.; Drain, C. M. *Langmuir* **2004**, *20*, 3974.
(20) Li, L.-L.; Yang, C.-J.; Chen, W.-H.; Lin, K.-J. *Angew. Chem., Int. Ed.* **2003**, *42*, 1505.
(21) (a) Liu, B.; Qian, D.-J.; Chen, M.; Wakayama, T.; Nakamura, C.; Miyake, J. *Chem. Commun.* **2006**, 3175. (b) Wang, Z.; Medforth, C. J.; Shelnutt, J. A. *J. Am. Chem. Soc.* **2004**, *126*, 15954. (c) Wang, Z.; Medforth, C. J.; Shelnutt, J. A. *J. Am. Chem. Soc.* **2004**, *126*, 16720. (d) Matsui, H.; MacCuspie, R. *Nano Lett.* **2001**, *1*, 671.
(22) (a) Barber, D. C.; Freitag-Beeston, R. A.; Whitten, D. G. *J. Phys. Chem.* **1991**, *95*, 4074. (b) Maiti, N. C.; Mazumdar, S.; Periasamy, N. *J. Phys. Chem. B* **1998**, *102*, 1528.
(23) (a) Kosal, M. E.; Chou, J.-H.; Wilson, S. R.; Suslick, K. S. *Nat. Mater.* **2002**, *1*, 118. (b) Suslick, K. S.; Bhyrappa, P.; Chou, J.-H.; Kosal, M. E.; Nakagaki, S.; Smithenry, D. W.; Wilson, S. R. *Acc. Chem. Res.* **2005**, *38*, 283.
(24) Yamaguchi, T.; Ishii, N.; Tashiro, K.; Aida, T. *J. Am. Chem. Soc.* **2003**, *125*, 13934.
(25) (a) Medforth, C. J.; Senge, M. O.; Smith, K. M.; Sparks, L. D.; Shelnutt, J. A. *J. Am. Chem. Soc.* **1992**, *114*, 9859. (b) Retsek, J. L.; Drain, C. M.; Kirmaier, C.; Nurco, D. J.; Medforth, C. J.; Smith, K. M.; Sazanovich, I. V.; Chirvony, V. S.; Fajer, J.; Holten, D. *J. Am. Chem. Soc.* **2003**, *125*, 9787.
(26) Harada, R.; Mastuda, Y. Okawa, H.; Kojima, T. *Angew. Chem., Int. Ed.* **2004**, *43*, 1825.
(27) Liu, C.-J.; Yu, W.-Y.; Peng, S.-M.; Mak, T. C. W.; Che, C.-M. *J. Chem. Soc., Dalton Trans.* **1998**, *11*, 1805.

Table 1. Crystallographic Data for 2

empirical formula	$C_{95.63}H_{60}N_4O_{9.75}Mo_3$
formula weight	1708.80
crystal system	monoclinic
space group (No.)	*C*2/c (No. 15)
T, K	123(2)
a, Å	21.496(4)
b, Å	30.230(6)
c, Å	25.858(5)
β, deg	104.85(3)
V, Å^3	16 242(6)
Z	8
D_c, g cm^{-3}	1.398
μ (Mo Kα), cm^{-1}	2.58
reflns measured	65 896
unique reflns, R_{int}	17 688, 0.0294
R[a]	0.064
Rw[b]	0.133
R1[c]	0.061 [$I > 2\sigma(I)$]
GOF	1.18

[a] $R = \sum(F_o^2 - F_c^2)/\sum F_o^2$. [b] $Rw = [\sum w(F_o^2 - F_c^2)^2/\sum w(F_o^2)^2]^{1/2}$. [c] $R1 = \sum||F_o| - |F_c||/\sum|F_o|$.

were prepared by the vapor diffusion of methanol to a toluene solution of **1** for 1 week. This method was reproducible for providing **2**. Elem anal. Calcd for $C_{102.5}H_{77}N_4O_{10}Mo_3$: C, 67.92; H, 4.28; N, 3.09. Found: C, 68.36; H, 4.44; N, 3.38.

Physical Measurements. UV−vis spectra were measured in a 1 cm quartz cell on a Shimadzu UV-3100PC UV−vis−NIR spectrophotometer in CH_2Cl_2 at room temperature. IR spectra were recorded on a Perkin-Elmer Spectrum BX FT-IR system with samples as KBr disks. All NMR measurements were carried out on JEOL GX-400 and EX-270 spectrometers. Electron Spin Resonance (ESR) spectra were recorded on a JEOL JES-FE3X spectrometer operating at X-band frequencies in CH_2Cl_2 at room temperature. A solid-state absorption spectrum of **2** was obtained by using a KBr pellet in transparent mode on a Jasco V-570 spectrophotometer. Fast-atom bombardment mass spectrometry (FAB-MS) spectra were recorded on a JMS-SX/SX102A Tandem mass spectrometer. The electric conductivity of **2** was measured by a conventional quasi-four-probe method using porous gold paint (Tokuriki Chemical Research, SILBEST No. 8560) and gold wire (25 mm f) with a Solatron SI 1260 impedance/gain-phase analyzer and a 1296 dielectric interface, at 1 kHz, under relative humidity from 38 to 81%, and at 300 K.

X-ray Crystallography on 2. A single crystal of **2** was obtained by recrystallization of **1** from toluene with vapor diffusion of methanol. The crystal was mounted on a glass fiber with silicon grease. The X-ray diffraction data for **2** were collected on a Rigaku/MSC mercury diffractometer with graphite monochromated Mo Kα radiation (λ = 0.710 70 Å) at 183 K. All data were refined anisotropically by the full-matrix least-squares method on F^2 for non-hydrogen atoms (SHELXL-97).[28] The hydrogen atoms were generated geometrically. Details of the crystal parameters, data collection, and refinements are summarized in Table 1.

TEM and High-Resolution TEM (HRTEM). TEM and HR-TEM images were obtained using a fully automated transmission electron microscope, TECNAI-20, FEI (acceleration voltage 200 kV). A porphyrin nanotube solution in methanol was dropped on a copper TEM grid with a commercial holey carbon support film. The excess amount of the solvent was then dried by using a Kimwipe tissue underneath. The TEM grid was dried further in the air overnight prior to loading into the vacuum chamber of the transmission electron microscope.

(28) Sheldrick, G. M. *SHELX97, Programs for Crystal Structure Refinement*; University of Göttingen: Göttingen, Germany, 1997.

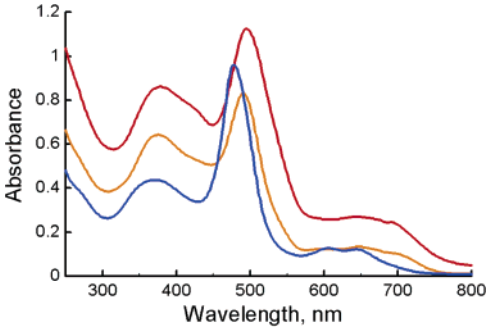

Figure 1. UV−vis spectra for **1** (blue line) and **2** (orange line) in CH_2Cl_2 and solid-state absorption spectrum of **2** (red line) in a KBr pellet.

Energy-Dispersive X-ray (EDX) Spectroscopy. EDX analysis was applied to investigate the presence of molybdenum from the porphyrin nanotubes containing Mo−oxo clusters. EDX spectra and EDX line-scan profiles were obtained from the nanotube and/or nanoring bridge over the hole. EDX spectra and EDX line scan profiles were also obtained by the same transmission electron microscope as for the image observation, TECNAI-20, FEI.

Results and Discussion

Synthesis of [Mo(DPP)(O)(OCH$_3$)] (1) and the Porphyrin Nanotube. This complex was prepared in 41% yield by the reaction of $[Mo(O)_2(acac)_2]$ (acac = acetylacetonato) with H_2DPP in phenol at 240 °C, followed by column chromatography on alumina and silica gel. The reaction temperature was adjusted to avoid the decomposition of H_2-DPP. The reaction of $Mo(CO)_6$ with H_2DPP in decalins gave no products, resulting in decomposition of the porphyrin. In the case of $MoCl_5$ as a starting material, the reaction with H_2DPP afforded **1** in only <3% yield, and almost all the porphyrin was recovered as H_4DPP^{2+}. Those starting materials have been valid for the synthesis of various Mo−TPP complexes (TPP = tetraphenylporphyrinato); however, it was revealed to be ineffective for those of Mo−DPP complexes.

The complex **1** showed the Soret and Q bands at 477, 605, and 642 nm in CH_2Cl_2 as shown in Figure 1. The ESR spectrum of **1** in CH_2Cl_2 at room-temperature exhibited a signal at g = 1.967 with superhyperfine structures due to four nitrogen nuclei ($A_N = 1.997 \times 10^{-4}$ cm^{-1}). The superhyperfine coupling constant for the nitrogen nuclei was smaller than that for [Mo(TPP)(O)(OMe)] ($A_N = 2.252 \times 10^{-4}$ cm^{-1})[29] in benzene, indicating weaker interactions between the Mo(V) center and DPP^{2-} due to saddle distortion. In its infrared (IR) spectrum (KBr method), a peak assigned to ν (Mo═O) was observed at 911 cm^{-1}.

Crystal Structure of the Porphyrin Nanotube. Recrystallization of **1** from toluene with vapor diffusion of MeOH for 1 week gave green crystals of a new compound, which was clearly different from the starting material **1**. X-ray crystallography of the new compound **2** revealed that the complex contained $[Mo(O)(DPP)(H_2O)]^+$, in which the methoxo ligand in **1** was replaced by H_2O and the complex had a +1 charge. The new Mo−DPP complex was crystallized in a monoclinic space group *C*2/*c* with the center of symmetry at tetranuclear Mo−oxo clusters. The crystal structure of the Mo-DPP moiety of **2**, $[Mo(O)(DPP)(H_2O)]^+$, is depicted in Figure 2, and selected bond lengths (Å) and angles (deg) are listed in Table 2.

(29) Matsuda, Y.; Murakami, Y. *Coord. Chem. Rev.* **1988**, *92*, 157.

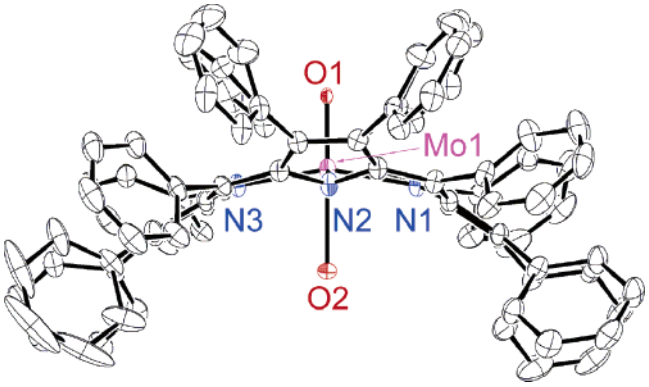

Figure 2. ORTEP drawing of the Mo−DPP moiety of **2** with 50% probability thermal ellipsoids. Hydrogen atoms are omitted for clarity.

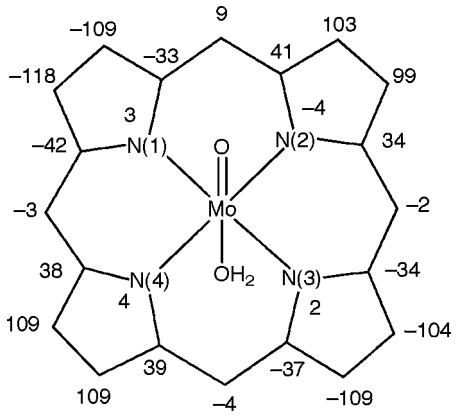

Figure 3. Displacements of 24 atoms from the porphyrin mean plane (in units of 0.01 Å).

Table 2. Selected Bond Lengths (Å) and Angles (deg) for 2

Mo1−O1	1.672(2)	Mo1−O2	2.340(2)
Mo1−N1	2.092(3)	Mo1−N2	2.087(3)
Mo1−N3	2.101(3)	Mo1−N4	2.078(3)
O1−Mo1−O2	179.0(1)	O1−Mo1−N1	101.1(1)
O1−Mo1−N2	99.6(1)	O1−Mo1−N3	99.9(1)
O1−Mo1−N4	100.4(1)		

As can be seen in Figure 2, the porphyrin ligand exhibited a large saddle distortion as reflected on displacement of each atom of the equatorial mean plane as shown in Figure 3. Bond lengths of Mo1−O1 and Mo1−O2 were determined to be 1.672(2) Å and 2.340(2) Å, respectively. These values indicate that Mo1−O1 should be Mo═O and Mo1−O2 should be Mo−OH_2 which was lengthened due to the strong trans influence of the strongly bound Mo═O moiety. The Mo═O bond length is in the range of those reported so far (1.71−1.64 Å).[30] The Mo−OH_2 bond is longer than that (2.093(3) Å) in [Mo(O)(TPP)(H_2O)]ClO_4 **(3)**, in which the aqua ligand is bound to ClO_4^- via hydrogen bonds,[31] but comparable to that (2.268(5) Å) in [Mo(NMe)(TPP)(H_2O)]-[I_3].[32] Bond distances among the Mo center and four porphyrin nitrogen atoms were 2.092(3) Å for Mo1−N1, 2.087(3) Å for Mo1−N2, 2.101(3) Å for Mo1−N3, and 2.078(3) Å for Mo1−N4, respectively.

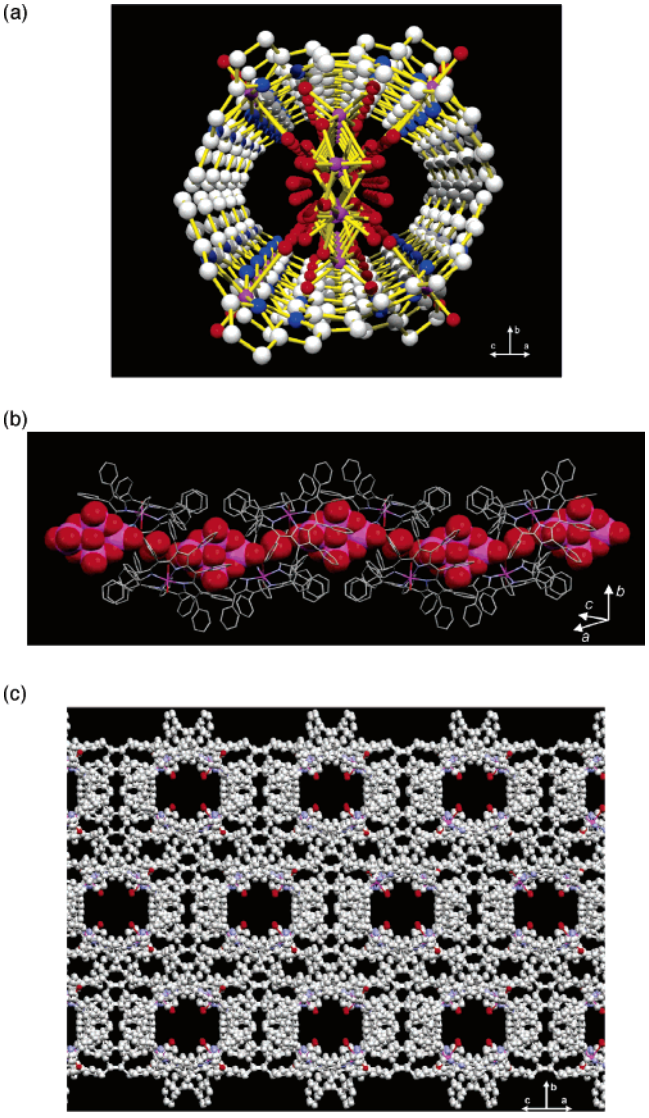

Figure 4. Crystal structure of the porphyrin nanotube; a sliced picture (a) (peripheral phenyl groups are omitted for clarity), a side view (b), and crystal packing (c) (Mo-oxo clusters and water molecules inside the tube are omitted for clarity).

The sliced picture of the crystal structure of the porphyrin nanotube is shown in Figure 4a, and the side view of the nanotube can also be seen in Figure 4b. The nanotubes are ordered in one direction to be perpendicular to the crystallographic *b* axis. The complex **2** directed the oxo group to the outside of the tube, and the aqua ligand was oriented toward the inside of the tube. This orientation allows us to obtain a nanosized *hydrophilic* environment in its inside to facilitate inclusion of hydrophilic entities such as Mo-oxo clusters inside of *hydrophobic* porphyrin aggregates. In the inner sphere of the tubular assembly of **2**, the aqua ligand forms intermolecular hydrogen bonding among an oxygen atom of the Mo−oxo cluster(s) and a water molecule of crystallization. This hydrogen bonding can contribute to stabilize the porphyrin nanotube and align the aggregation in the order. The tubular assembly is derived from intermolecular $\pi-\pi$ interactions of alternatively inserted peripheral phenyl groups, for which the ring−ring distances fall in the range of 3.46−3.74 Å. This feature is unprecedented in porphyrin aggregation. In the J-aggregates, which are the most common mode of porphyrin superstructures, porphyrin

(30) Ohkubo, Y.; Okamura, A.; Imanishi, K.; Tachibana, J.; Umakoshi, K.; Sasaki, Y.; Imamura, T. *Bull. Chem. Soc. Jpn.* **1999**, *72*, 2241.
(31) Hamstra, B. J.; Cheng, B.; Ellison, M. K.; Scheidt, W. R. *Inorg. Chem.* **1999**, *38*, 3554.
(32) Kim, J. C.; Rees, W. S., Jr.; Goedken, V. L. *Inorg. Chem.* **1995**, *34*, 2483.

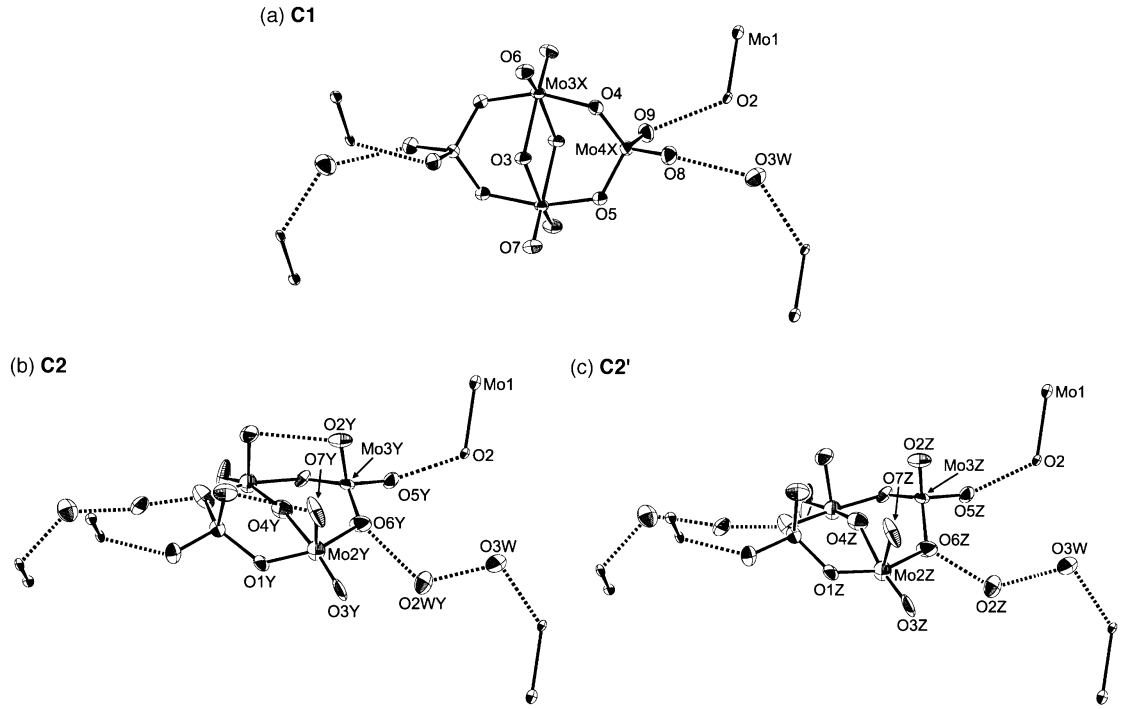

Figure 5. ORTEP drawings of tetranuclear Mo−oxo clusters with 50% probability thermal ellipsoids.

Scheme 2. Schematic Description of the Nanotube Formation with Curved Surfaces Concomitant with the Size-Selective Inclusion of Mo(VI)−Oxo Clusters

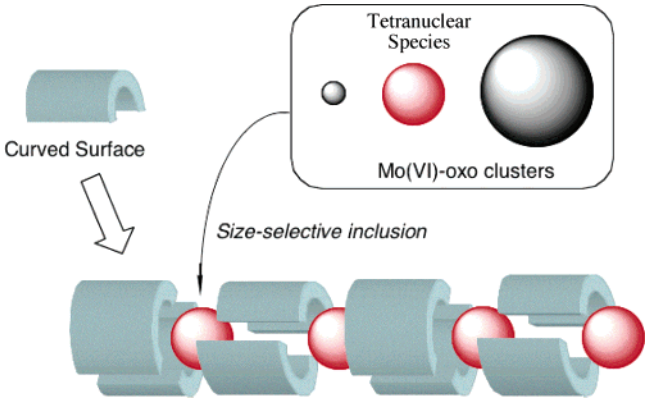

surfaces stack with each other to undergo $\pi-\pi$ interactions with offsets.

In the crystal, no direct interaction was observed between the porphyrin nanotubes. However, toluene molecules of crystallization acted as an adhesive to associate the tubes together by virtue of intermolecular $\pi-\pi$ and CH/π interactions. As described above, the tubes aligned to be perpendicular to the crystallographic *b* axis, exhibiting an ordered channel structure as shown in Figure 4c. This structural motif is reminiscent of inorganic zeolites.

The Mo−oxo clusters incorporated into the tube were revealed to possess three kinds of unique structures. Their ORTEP diagrams and corresponding schematic descriptions with bond distances (Å) are depicted in Figures 5 and 6, respectively. Populations of those clusters were estimated to be 0.8 for **C1**, 0.1 for **C2**, and 0.1 for **C2′** in the X-ray crystallography. All of the clusters possess unprecedented discrete structural motifs with only oxo and hydroxo bridges and terminal oxo groups without any organic moieties. In

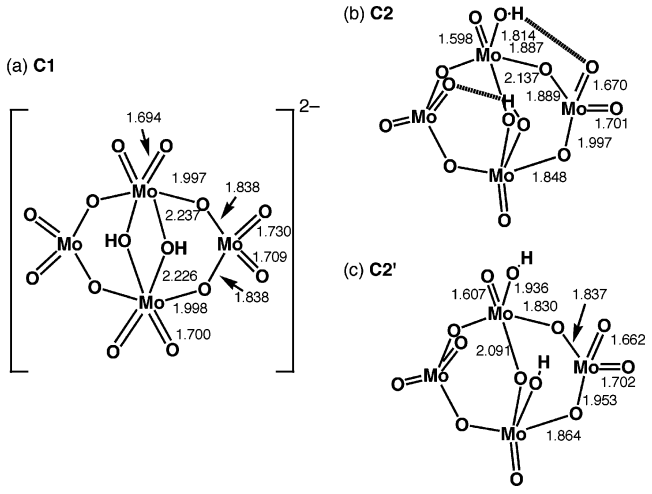

Figure 6. Schematic descriptions of the tetranuclear Mo−oxo clusters with bond distances (Å).

the case of **C1**, two μ-hydroxo and four μ-oxo bridges linked two octahedral and two tetrahedral Mo(VI) centers. No metal−metal interaction is recognized based on interatomic distances (>3 Å). This structural motif has been found in Mo−oxo clusters with hydrazido and diazenido groups instead of the terminal oxo moieties as reported by Zubieta and co-workers.[33,34] Clusters **C2** and **C2′** were revealed to have two terminal hydroxo and one μ-oxo groups. Short Mo═O and Mo−OH bond lengths and the lack of Mo··· Mo bonding interaction suggest that all the four Mo centers are Mo(VI) as in **C1** rather than in mixed-valent states. In sharp contrast to **C1**, the clusters of **C2** and **C2′** consist of two tetrahedral and two pseudo-square-pyramidal geometries. Thus, the clusters **C2** and **C2′** are probably neutral species,

(33) (a) Shaikh, S. N.; Zubieta, J. *Inorg. Chem.* **1986**, *25*, 4613. (b) Hsieh, T.-C.; Shaikh, S. N.; Zubieta, J. *Inorg. Chem.* **1987**, *26*, 4079.
(34) See also: (a) Kahn, M. I.; Zubieta, J. *Prog. Inorg. Chem.* **1995**, *43*, 1. (b) Gouzerh, P.; Proust, A. *Chem. Rev.* **1998**, *98*, 77.

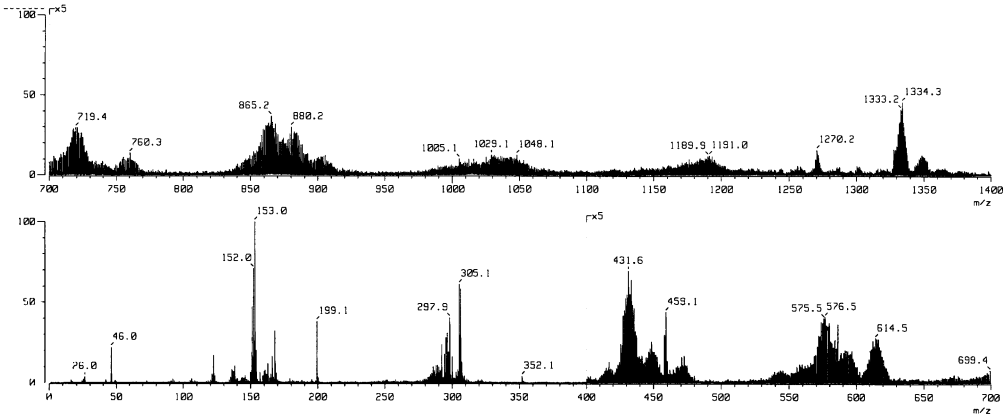

Figure 7. FAB-MS (negative-mode) spectrum of **2** observed in 3-nitrobenzyl alcohol.

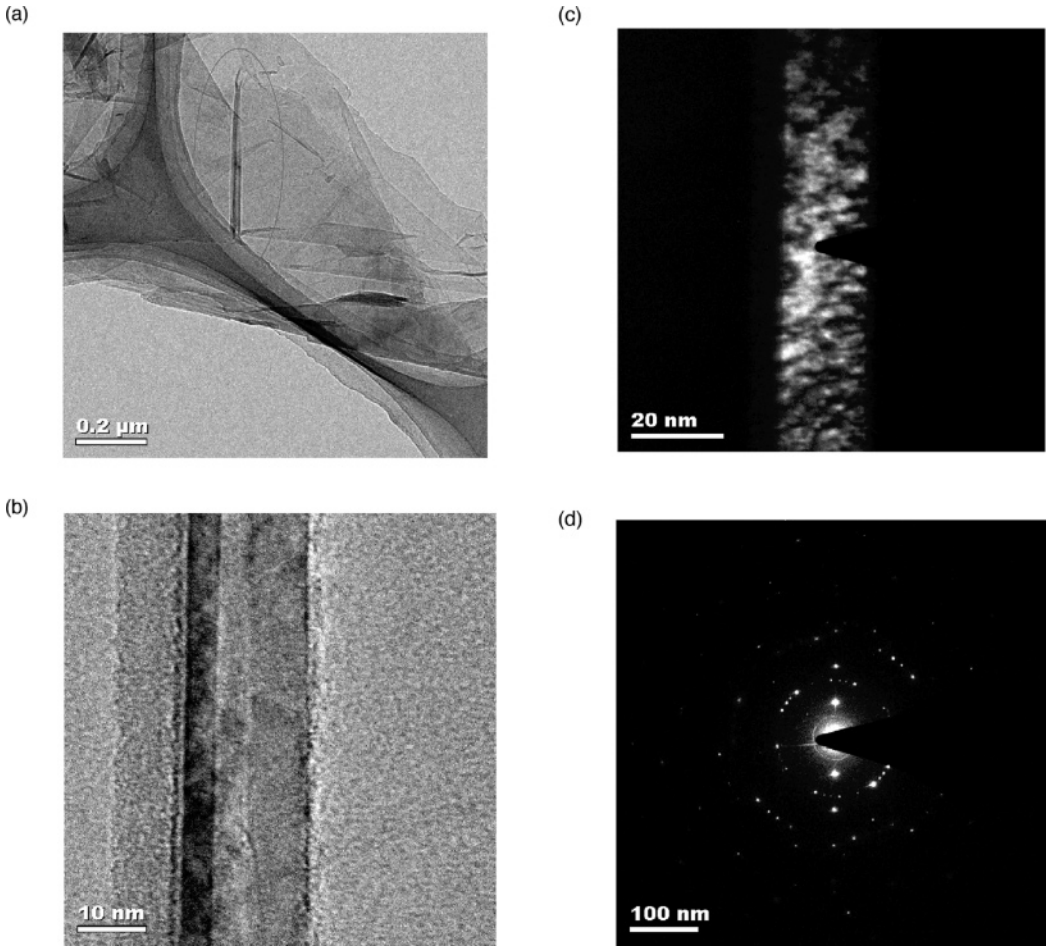

Figure 8. TEM observations on the porphyrin nanotube: TEM images of a porphyrin nanotube supported on the copper grid (a) and its magnified image (b), the dark-field image (c), and the electron diffraction (d).

and one of two water molecules of crystallization shown in Figure 5b,c could be formally hydroxide (OH^-). **C2** and **C2′** can be intermediates for larger Mo−oxo aggregates, but they are stabilized and protected by shielding of the hydrophobic porphyrin nanotube. The included Mo(VI)−oxo clusters are all tetranuclear because they are favorable in size so as to be included within the tube of 1-nm diameter. We assume that those tetranuclear clusters could be formed and protected in accordance with the porphyrin aggregation in the hydrophilic cavity, and they could also act as templates for the tube to be stabilized. Schematic description of the porphyrin nanotube formation is given in Scheme 2. Previously, Zubieta and co-workers also reported on encapsulation of $[Mo_6O_{19}]^{2-}$ into a three-dimensional infinite framework consisting of $[Fe_8(\text{tetrapyridylporphyrin})_6]^{8+}$ as a building block, which was synthesized by hydrothermal reaction.[35] In their cases, the microporous structures made by porphyrin complexes could provide a cavity for a "ship-in-a-bottle" synthesis of those metal clusters, and no interaction between the metal center of porphyrin complexes and the metal cluster was included. In contrast to this, our porphyrin nanotube can be

(35) Hagrman, D.; Hagrman, P. J.; Zubieta, J. *Angew. Chem., Int. Ed.* **1999**, *38,* 3165.

a result of cooperative formation of the tetranuclear Mo−oxo clusters and discrete tubular assembly of $[Mo(DPP)(O)(H_2O)]^+$ by virtue of noncovalent interactions.

Proton Conductivity of a Single Crystal of 2. We examined proton conductivity of a single crystal of the porphyrin nanotube **2** under controlled relative humidity. Measurements were carried out at ambient temperature with an impedance analyzer. DC electrical conductivity of **2** was measured to be $<10^{-13}$ S cm^{-1}, indicating that **2** is an insulator. On the contrary, AC electrical conductivity of **2** at 1 kHz was found to be 3×10^{-9} S cm^{-1} under relative humidity of 81% as shown in Figure S1 (Supporting Information). These results indicate ion-conductive nature of **2**, which is induced by proton conduction probably through the hydrogen-bonded network, consisting of water molecules and the Mo−oxo clusters, within the nanotube.

Solid-State Absorption Spectra. In order to gain insights into the mode of aggregation in the porphyrin nanotube, we measured a reflection spectrum of **2** in a KBr pellet. As can be seen in the spectrum in Figure 1 (red line), the absorption maxima are observed at 380, 495, 644, and 691 nm, which are virtually identical to those in solution (orange line in Figure 1). Thus, the solution structure of **2** is essentially the same as that in the solid state. This indicates that $[Mo(DPP)(O)(H_2O)]^+$ exhibits the same electronic structure in both states and behaves as ion pairs.

FAB-MS Spectroscopy. In the negative-mode FAB-MS spectrum for the crystals of **2** using 3-nitrobenzyl alcohol as a matrix, a number of peak clusters were observed due to formation of a number of Mo−oxo clusters with a variety of nuclear numbers, as depicted in Figure 7. This indicates that the Mo−oxo clusters included in the nanotube can dissociate and associate to change their sizes and shapes. The selectivity of tetranuclear clusters can be determined in the course of the formation of the nanotube: Many local energy minima could exist corresponding to clusters with certain nuclear numbers whereas the tetranuclear clusters should be the global minimum(s) in terms of the size to fit the inner space of the nanotube.

On the basis of this observation, we assumed that the size of the porphyrin nanotube could be controlled by the size of the Mo-oxo cluster included. Thus, we examined larger sizes of the porphyrin nanotubes with the aid of TEM as described in the following section.

TEM Observations. We applied TEM to directly observe the formation of larger-sized porphyrin nanotubes. Figure 8a shows a straight nanotube to exemplify the formation of the larger-sized nanotubes and the expanded image of the nanotube with ca. 20 nm in diameter is depicted in Figure 8b. Electron diffraction and EDX spectra confirm that the nanotube observed is composed of molybdenum and oxygen. The dark-field image (Figure 8c) and electron diffraction (Figure 8d) indicate the existence of Mo clusters as polycrystals. On the basis of the EDX analysis, the distribution of the Mo centers exhibits ∼20 nm as shown in Figure 9. Other tubular motifs were observed by TEM as shown in Supporting Information. This indicates that the larger-sized nanotube is not accidentally found but generally observed.

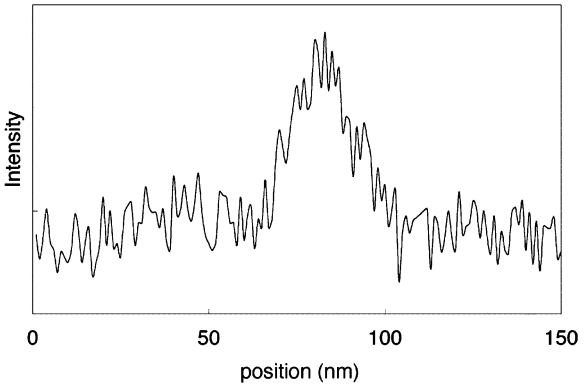

Figure 9. EDX spectroscopy profile based on the Mo-L edge absorption.

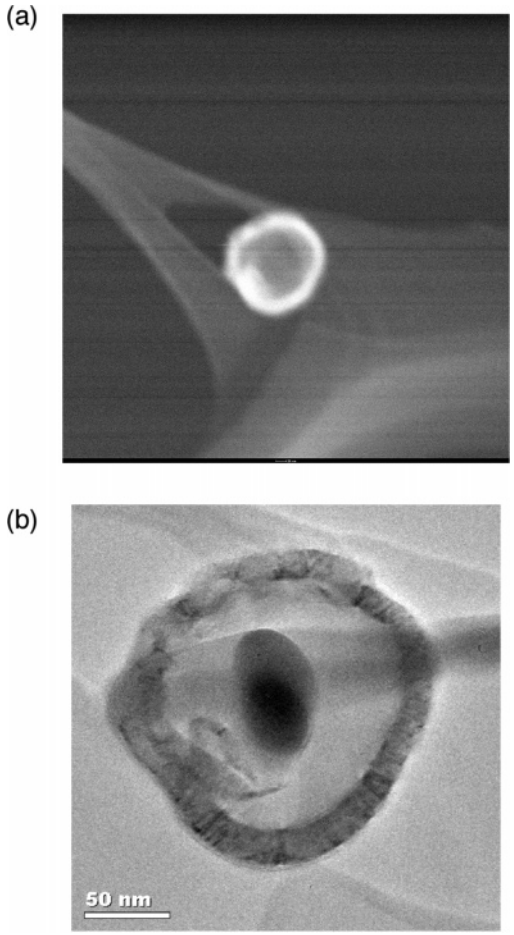

Figure 10. TEM observations of the porphyrin nanoring: a dark-field image (a) and TEM image (b). In part b, the black line and the black spot of the center of the ring are the result of a scar of EDX analysis.

In addition, we have also observed the formation of a "porphyrin nanoring", which exhibited the diameter of almost 200 nm and the tubular assembly with 20-nm diameter as shown in Figure 10. The EDX analysis of this ring confirmed that molybdenum and oxygen are also present within this nanoring. The size of the nanoring is far larger than that one can expect (∼15 nm) from self-assembly of the tetra(*p*-carboxyphenyl)porphyrin dication (H_2TCPP^{2+}).[36]

Conclusion

A saddle-distorted Mo(V)−dodecaphenylporphyrinato complex **2** forms nanoscaled tubular structures via self-assembly

by virtue of intermolecular $\pi-\pi$ interactions among peripheral phenyl moieties and intermolecular hydrogen bonding with tetranuclear Mo(VI)−oxo clusters as template molecules. A remarkable feature of the tubular assembly presented here is the formation of the hydrophilic isolated inner sphere in the hydrophobic porphyrin supramolecule. This concept provides us an idea for the isolation and protection of unusual and unstable entities formed in the course of the formation of porphyrin assemblies with saddle-distorted nonplanar porphyrins as building blocks. Our strategy to use the saddle-distorted porphyrin complexes as curved surfaces to construct supramolecular assemblies give novel aggregation modes other than typical J-aggregation for planar porphyrins and metalloporphyrins, due to steric effects of the distortion. Novel aggregation modes due to curved surfaces allow us to access a variety of new assemblies of metalloporphyrins toward innovation of porphyrin-based functional materials.

Acknowledgment. We would like to thank Prof. Masaki Kawano (Graduate School of Engineering, The University of Tokyo) and Dr. Yuichi Shimazaki (Institute for Materials Chemistry and Engineering, Kyushu University) for their help in X-ray crystallography. This work has been supported by Grants-in-Aid (Nos. 16550057 and 18033033) from the Ministry of Education, Culture, Sports, Science and Technology of Japan and a Grant from Iketani Science and Technology Foundation.

Supporting Information Available: Crystallographic data (CIF) for **2**, time-course of conductivity of **2**, and additional TEM images. This material is available free of charge via the Internet at http://pubs.acs.org.

CM062031K

(36) Doan, S. C.; Shanmugham, S.; Aston, D. E.; McHale, J. L. *J. Am. Chem. Soc.* **2005**, *127*, 5885.